



## Electroless Synthesis of Pure Nickel Metal Nanotubes Using Silicon Oxide Nanowires as Removable Templates

S. L. Cheng<sup>a,b,z</sup> and W. C. Hsiao<sup>b</sup>

<sup>a</sup>Department of Chemical and Materials Engineering, and <sup>b</sup>Institute of Materials Science and Engineering, National Central University, Chung-Li City, Taoyuan, Taiwan

We report here the first successful synthesis of pure Ni nanotubes by employing the electroless Ni deposition in conjunction with removable amorphous SiO<sub>x</sub> (a-SiO<sub>x</sub>) nanowire templates technique. After the 3-aminopropyltrimethoxysilane (APTMS) functionalization, activation, and hydrazine-modified electroless Ni plating processes, a uniform a-SiO<sub>x</sub>/pure Ni core-shell nanowire structure is produced. By etching away the inner a-SiO<sub>x</sub> nanowire templates, hollow Ni nanotubes are readily obtained. The observed results present the exciting prospect that with appropriate controls, the hydrazine-modified electroless deposition combined with the APTMS-functionalized a-SiO<sub>x</sub> nanowire templates technique can be successfully implemented in forming a variety of high-purity, hollow, metal nanotubes.

© 2007 The Electrochemical Society. [DOI: 10.1149/1.2790277] All rights reserved.

Manuscript submitted July 18, 2007; revised manuscript received September 4, 2007. Available electronically October 9, 2007.

As the device dimensions scale down to the nanometer region, advanced nanoscale fabrication technology is expected to play a key role in the applications of future nanodevices. Recently, studies of one-dimensional (1D) metal nanostructures with hollow interiors (i.e., nanotubes) have drawn much attention, because 1D metallic nanotubes have already found potential applications in advanced optoelectronics, catalysts, chemical sensors, and magnetic data storages.<sup>1-5</sup> However, compared with the fabrication processes of 1D nanowires, the syntheses of 1D nanotubes are relatively complex and difficult due to the characteristic hollow-tube structures. Therefore, many recent research efforts have been dedicated to the large-scale syntheses of the 1D metal nanotubes.<sup>6-10</sup> Among these approaches, the electroless deposition of metal in conjunction with removable nanoscale templates technique is one of the most promising schemes for synthesizing metallic nanotubes.

In these template synthesis methods, amorphous silicon oxide (a-SiO<sub>x</sub>) nanowires are perhaps the most promising materials that can be used as the sacrificial templates because they possess a smooth surface, high aspect ratio, and good thermal stability. In addition, the a-SiO<sub>x</sub> nanowires can be easily removed. As for the deposition of desired metal thin films onto the surfaces of the a-SiO<sub>x</sub> nanowire templates, electroless plating is a low-cost, high-throughput, and effective technique. Previous studies have reported that electroless nickel film was widely used for many industrial applications due to its unique chemical, magnetic, and mechanical properties.<sup>11-14</sup> Recently, it has been demonstrated that by employing the templating methods and electroless plating techniques, 1D nickel metal nanotubes can be synthesized.<sup>15,16</sup> However, from the chemical reducing agents, such as dimethylamine borane or sodium hypophosphite, used in these studies, a dramatic amount of impurities (e.g., boron or phosphorus) were found to form in the electroless Ni layers. For microelectronic applications, these impurities would lead to an increase in the electrical resistivity of synthesized Ni films as well as degradation in the reliabilities of lead-free solder joints.<sup>17-19</sup> Therefore, in order to reduce the above-mentioned drawbacks, the routes for electroless synthesis of pure Ni plating on the surface of sacrificial templates are demanded.

In the present study, a facile route for the large-scale synthesis of high-purity hollow Ni nanotubes has been developed using the hydrazine-modified electroless Ni deposition processes with 3-aminopropyltrimethoxysilane (APTMS)-functionalized a-SiO<sub>x</sub> nanowires serving as sacrificial templates. The results from an investigation on the surface morphology, crystallinity, chemical composition, and microstructures of the synthesized 1D nickel nanotubes are reported.

### Experimental

A facile technique using a gold catalyst layer and high-temperature heat-treatment was utilized to synthesize the sacrificial a-SiO<sub>x</sub> nanowire templates on silicon substrates in this study. Single-crystal, p-type Si(001) wafers were cleaned chemically by a standard procedure, followed by dipping in a dilute hydrofluoric acid (HF) solution before loading into an electron-beam evaporation chamber. Thin Au metal films, 4 nm in thickness, were then deposited onto the cleaned Si(001) wafers in a vacuum at a base pressure lower than  $1 \times 10^{-7}$  Torr. The evaporated Au thin films served as the catalyst layers. Large-area silicon oxide nanowires were grown on the Au-catalyst-layer-coated Si substrates by thermal annealing in a three-zone diffusion furnace at 1000°C for 60 min. The as-synthesized a-SiO<sub>x</sub> nanowires were treated with a 5 mM toluene solution of APTMS for 180 min at room temperature to functionalize the surface of the a-SiO<sub>x</sub> nanowires. After rinsing with deionized (DI) water, the amine-group-functionalized a-SiO<sub>x</sub> nanowires were activated by immersing the samples in an aqueous solution containing 0.3 g/L PdCl<sub>2</sub> and 6.25 mL/L HCl for 10 min. The prepared a-SiO<sub>x</sub> nanowires were used as templates for the electroless deposition of pure Ni.

For the electroless plating processes, the activated a-SiO<sub>x</sub> nanowire templates were immersed into the electroless nickel plating baths at 60°C for 3 min. The electroless plating solution was composed of 0.07 M nickel acetate tetrahydrate [Ni(CH<sub>3</sub>COO)<sub>2</sub>·4H<sub>2</sub>O] as the Ni metal source and 0.2 M hydrazine (N<sub>2</sub>H<sub>4</sub>·H<sub>2</sub>O) as the chemical reducing agent. The pH value of the plating solution was adjusted to  $9.0 \pm 0.1$  by the addition of ammonium hydroxide (NH<sub>4</sub>OH) solution. The Ni ions were reduced to Ni and then deposited onto the surface of the a-SiO<sub>x</sub> nanowires to form a continuous pure Ni nanoshell. The pure Ni-coated a-SiO<sub>x</sub> nanowire samples were thoroughly washed with DI water and dried with compressed air. Subsequently, the a-SiO<sub>x</sub>/pure Ni core-shell nanowires were transferred to a dilute HF solution. The core a-SiO<sub>x</sub> nanowire templates were etched away by a dilute HF rinse and the pure hollow Ni metal nanotubes were then obtained.

The morphologies of as-synthesized a-SiO<sub>x</sub> templates, a-SiO<sub>x</sub>/Ni core-shell nanowires, and resulting pure Ni metal nanotubes were examined using scanning electron microscopy (SEM, Hitachi S-3000H). Transmission electron microscopy (TEM, JEOL JEM2000FXII) and selected-area electron diffraction (SAED) analysis were carried out for microstructure determination and crystallography characterization. High-resolution TEM (HRTEM, JEOL JEM2100) and an energy-dispersion spectrometer (EDS) attached to the HRTEM were utilized to analyze the atomic structures and the chemical compositions of synthesized nanostructures, respectively.

<sup>z</sup> E-mail: slcheng@ncu.edu.tw

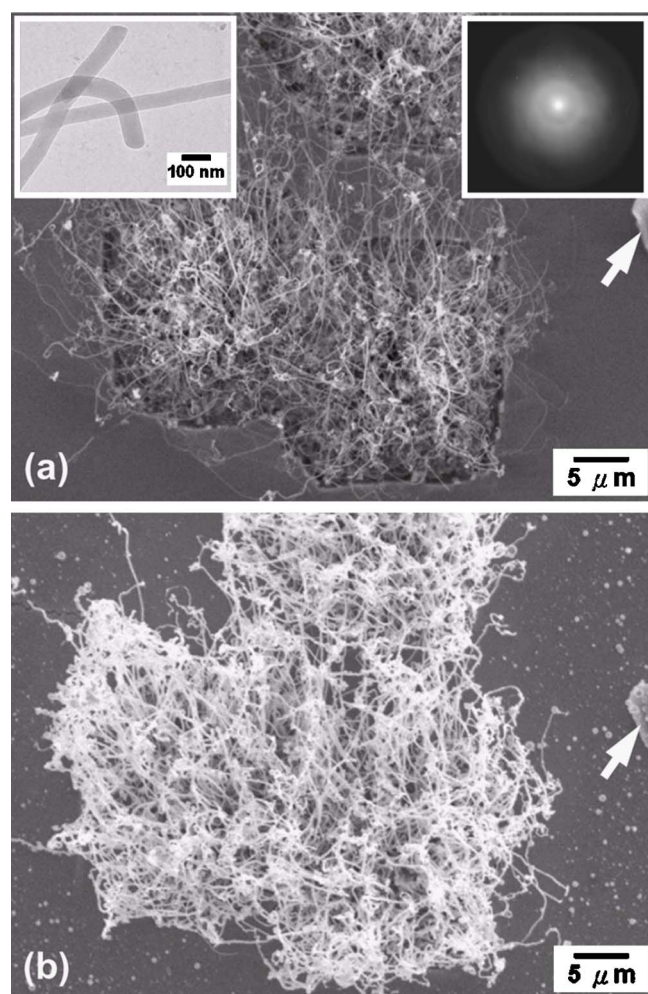


**Figure 1.** SEM images of the amorphous  $\text{SiO}_x$  nanowire templates (a) before and (b) after the modified electroless Ni deposition processes. The upper left and right insets of (a) show the high-magnification TEM image and the corresponding SAED pattern of the as-synthesized a- $\text{SiO}_x$  nanowires, respectively. (The white arrow points to the fiducial marker.)

### Results and Discussion

Figures 1a and b show SEM micrographs of the silicon oxide nanowire templates before and after electroless Ni plating. From Fig. 1a, it is clearly seen that dense  $\text{SiO}_x$  nanowires have been formed on the Au-coated Si(001) substrate after annealing at  $1000^\circ\text{C}$ . The length of the as-synthesized  $\text{SiO}_x$  nanowires was in the order of tens of micrometers. From TEM observation, the surfaces of all  $\text{SiO}_x$  nanowires were found to be smooth and clean. The diameters for most of these  $\text{SiO}_x$  nanowires were in the range of 30–150 nm. From SAED analysis, no diffraction rings or spots were detected in the diffraction pattern of the  $\text{SiO}_x$  nanowires, suggesting that the  $\text{SiO}_x$  nanowires are amorphous. The corresponding high-magnification TEM image and SAED pattern of the a- $\text{SiO}_x$  nanowires are shown in the left and right insets of Fig. 1a, respectively. Prior to the electroless deposition process, the a- $\text{SiO}_x$  nanowires were first functionalized with APTMS to generate an amine-moiety-coated surface. Subsequently, the a- $\text{SiO}_x$  nanowires were activated by immersing the samples into the  $\text{PdCl}_2$  solution. The Pd was chemiadsorbed onto the surfaces of APTMS-functionalized a- $\text{SiO}_x$  nanowires. These surface-modified silicon oxide nanowires were then used as the electroless Ni deposition templates. Figure 1b shows the SEM micrograph of the same region shown in Fig. 1a after electroless Ni deposition using hydrazine as the reducing agent. Compare with the as-synthesized a- $\text{SiO}_x$  nanowires (Fig. 1a), it is

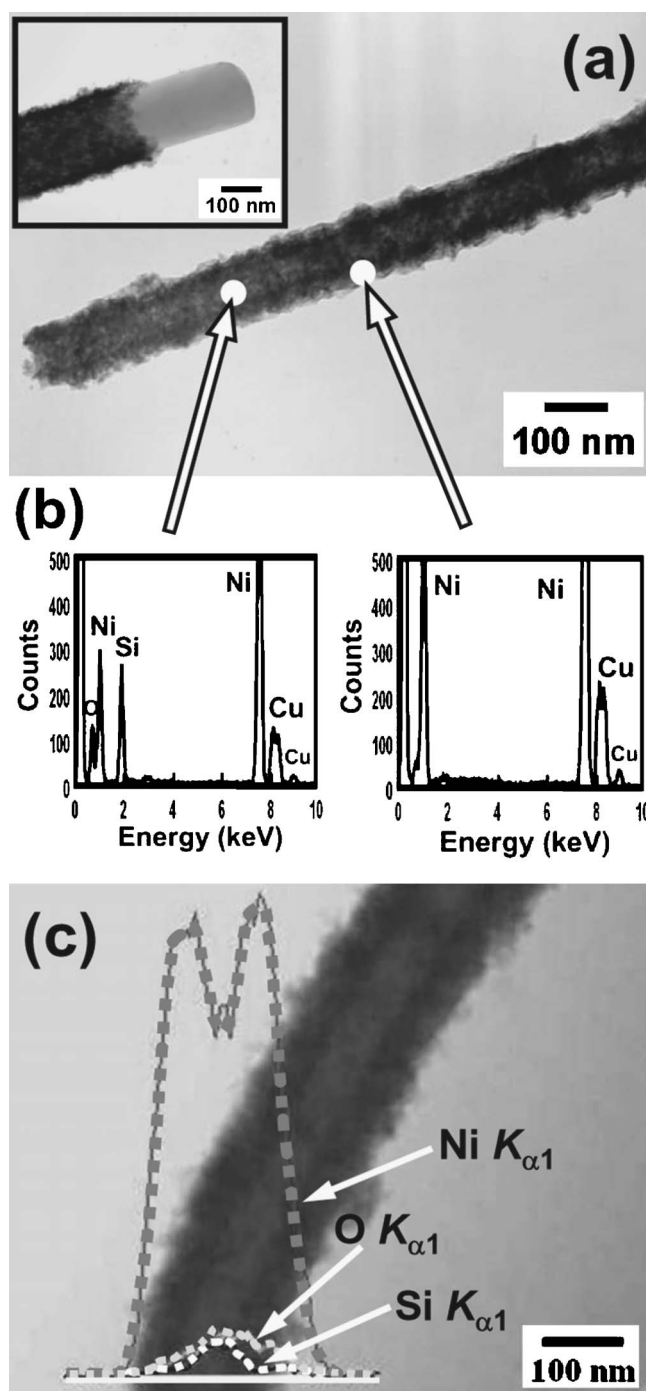


**Figure 2.** (a) TEM image of the surface-modified a- $\text{SiO}_x$  nanowire after electroless Ni deposition. The inset shows an a- $\text{SiO}_x$ /Ni coaxial nanowire structure. (b) Corresponding EDS spectra and (c) EDS linescan profiles of the a- $\text{SiO}_x$ /Ni core-shell nanostructures.

evident from Fig. 1b that the surface-modified a- $\text{SiO}_x$  nanowires were coated with a thin Ni layer after the electroless deposition. From TEM observation and EDS analysis, it is revealed that the as-deposited nanowire structure was composed of an a- $\text{SiO}_x$  inner core and a continuous Ni outer nanoshell. The corresponding TEM micrograph and EDS spectra of the as-prepared a- $\text{SiO}_x$ /Ni core-shell nanostructures are shown in Fig. 2a and b, respectively. The presence of Cu peaks in the EDS spectra can be attributed to the supporting copper grid used for TEM analysis. Figure 2c displays the EDS linescan profiles across the a- $\text{SiO}_x$ /Ni core-shell nanowire. The



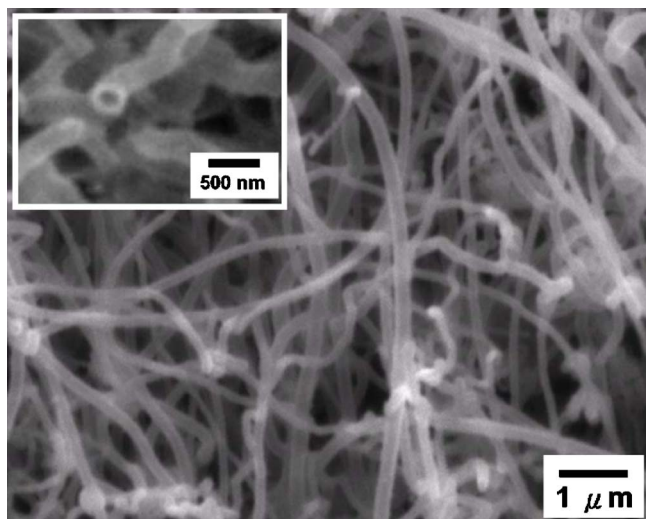


**Figure 3.** SEM image of the as-prepared hollow Ni nanotubes. The inset shows the SEM image of the open end of a Ni nanotube.

composition distribution is further confirmed by monitoring the change of X-ray signal from Ni, Si, and O atoms in the core-shell nanostructure.

Both the APTMS-functionalization and activation are key steps in the electroless deposition procedures. Electroless Ni deposition does not occur for the a-SiO<sub>x</sub> nanowire templates without functionalization and activation treatments. The possible deposition mechanisms for the modified electroless deposition have been proposed in previous studies.<sup>18,20-23</sup> Following the modified electroless Ni deposition, the core-shell nanowire samples were immersed into a dilute HF solution to remove the a-SiO<sub>x</sub> nanowire cores. The morphology

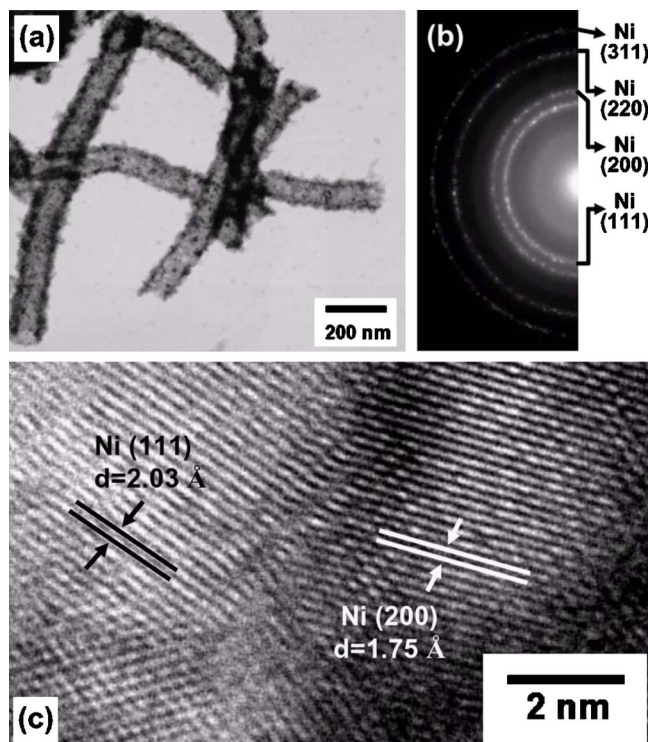


**Figure 4.** (a) TEM image and (b) corresponding SAED pattern of the Ni metal nanotubes. (c) HRTEM image taken at the edge of the Ni outer nanoshell in a pure hollow Ni nanotube.

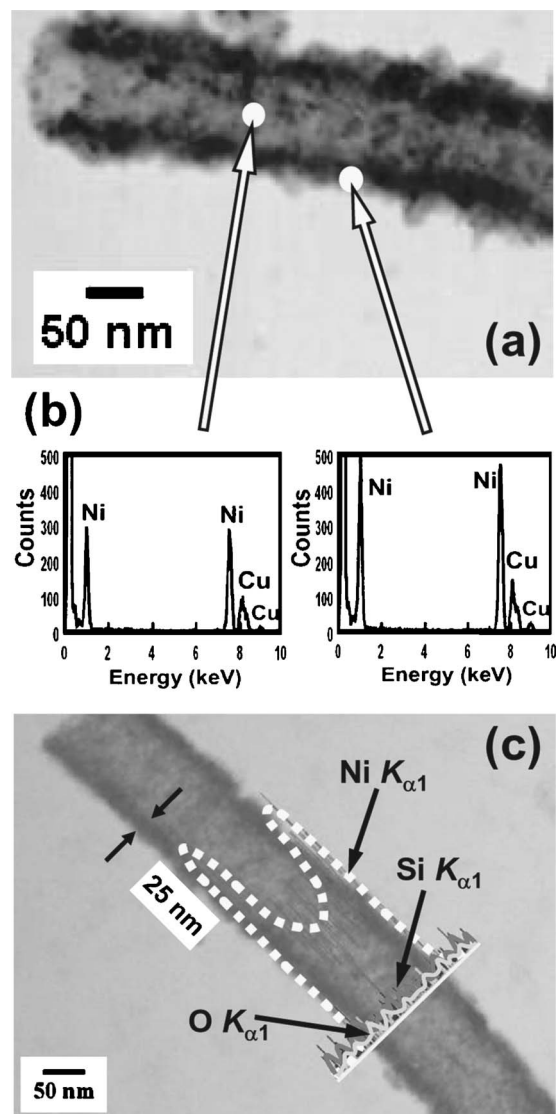


**Figure 5.** (a) TEM image and (b) corresponding EDS spectra of a pure hollow Ni nanotube. (c) EDS linescan profiles across a hollow Ni nanotube.

of the obtained tubular nanostructures is shown in Fig. 3. The shell thickness was found to be relatively uniform over the entire length. The inset of Fig. 3 shows the open end of a Ni nanotube. The microstructures and crystallinities of the obtained hollow Ni nanotubes were further examined by TEM, SAED, and HRTEM analysis. The TEM micrograph, as shown in Fig. 4a, revealed that the grain size and shell thickness of the hollow Ni nanotubes were about 8–10 and 25–30 nm, respectively. From SAED analysis, diffraction rings corresponding to the (111), (200), (220), and (311) diffractions of the face-centered-cubic (fcc) Ni phase were detected in the SAED pattern, indicating that the crystal structure of the prepared Ni nanotube was polycrystalline. An example is shown in Fig. 4b. Figure 4c shows the high-resolution TEM micrograph of a Ni nanotube which is a part magnification at the edge of the Ni outer shell. The measured lattice spacings of 0.203 and 0.175 nm are consistent with the interplanar spacing values for the (111) and (200) planes of a pure cubic Ni crystal, respectively.

Figures 5a and b show the TEM micrograph and the corresponding EDS spectra of a hollow Ni nanotube. The EDS analysis clearly demonstrated that the nanotubes were entirely composed of pure nickel. No Si and O signals were detected in the nanotube samples. Moreover, the distribution of the above-mentioned elements was

examined by the EDS linescan profile analysis as shown in Fig. 5c. The EDS linescan results further confirmed that the inner a-SiO<sub>x</sub> nanowire cores were completely removed by HF etching and the pure hollow Ni nanotubes were successfully synthesized.

Based on the SEM, TEM, and HRTEM observations and SAED and EDS analysis, the experimental results have clearly demonstrated that the a-SiO<sub>x</sub>/Ni core-shell nanowire structures and hollow Ni nanotubes were successfully synthesized using the a-SiO<sub>x</sub> nanowires as sacrificial cores combining the APTMS and hydrazine-modified electroless Ni deposition technique. The produced Ni nanotubes have high purity, smooth surface, and high crystallinity. The inner diameters of the Ni nanotubes are determined by the diameters of a-SiO<sub>x</sub> nanowire cores, while the thickness of the outer Ni nanoshell can be adjusted by tuning of the electroless deposition conditions.

### Conclusion

The present study has demonstrated that large quantities of pure hollow Ni nanotubes were first successfully synthesized using the electroless Ni deposition technique with APTMS-modified a-SiO<sub>x</sub> nanowires serving as removable templates. SEM and TEM images clearly reveal that the surface morphology of the synthesized Ni nanotubes was continuous and smooth. The inner diameters of the Ni nanotubes were about 30–150 nm, depending on the diameter of a-SiO<sub>x</sub> nanowire cores, and the thickness of outer Ni nanoshells was in the range of 25–30 nm. In the absence of APTMS-functionalization and activation treatments, the electroless Ni deposition onto the surface of a-SiO<sub>x</sub> nanowire templates did not occur. From SAED, EDS, and HRTEM analysis, it can be concluded that the prepared nanotubes were entirely composed of pure nickel and the crystal structure of the produced hollow Ni nanotube was polycrystalline.

The observed results present the exciting prospect that using high-aspect-ratio a-SiO<sub>x</sub> nanowires as the removable templates, the APTMS and hydrazine modified electroless deposition technique promises to be applicable to the large-scale synthesis of a variety of high-purity, hollow, metal nanotubes.

### Acknowledgment

This research was supported by the National Science Council through grant no. NSC 95-2221-E-008-021.

National Central University assisted in meeting the publication costs of this article.

### References

1. P. Kohli, C. C. Harrell, C. H. Cao, R. Gasparac, W. H. Tan, and C. R. Martin, *Science*, **305**, 984 (2004).
2. C. R. Martin, M. Nishizawa, K. Jirage, and M. Kang, *J. Phys. Chem. B*, **105**, 1925 (2001).
3. S. F. Yu, U. Welp, L. Z. Hua, A. Rydh, W. K. Kwok, and H. H. Wang, *Chem. Mater.*, **17**, 3445 (2005).
4. S. G. Jang, H. K. Yu, D. G. Choi, and S. M. Yang, *Chem. Mater.*, **18**, 6103 (2006).
5. B. I. Seo, U. A. Shaislamov, S. J. Lee, S. W. Kim, I. S. Kim, S. K. Hong, and B. Yang, *J. Cryst. Growth*, **292**, 315 (2006).
6. G. W. Xie, Z. B. Wang, G. C. Li, Y. L. Shi, Z. L. Cui, and Z. K. Zhang, *Mater. Lett.*, **61**, 2641 (2007).
7. H. Q. Cao, L. D. Wang, Y. Qiu, Q. Z. Wu, G. Z. Wang, L. Zhang, and X. W. Liu, *ChemPhysChem*, **7**, 1500 (2006).
8. Y. Sun, B. Mayers, and Y. Xia, *Adv. Mater. (Weinheim, Ger.)*, **15**, 641 (2003).
9. J. H. Wang, P. Y. Su, M. Y. Lu, L. J. Chen, C. H. Chen, and C. J. Chiu, *Electrochem. Solid-State Lett.*, **8**, C9 (2005).
10. N. Li, X. T. Li, X. J. Yin, W. Wang, and S. L. Qiu, *Solid State Commun.*, **132**, 841 (2004).
11. C. Guzman, N. Diaz, J. A. Berrios, A. Pertuz, and E. S. P. Cabrera, *Surf. Coat. Technol.*, **133-134**, 561 (2000).
12. R. C. Agarwala, V. Agarwala, and R. Sharma, *Synth. React. Inorg. Met.-Org. Nano-Metal Chem.*, **36**, 493 (2006).
13. R. W. Miles, B. Ghosh, S. Duke, J. R. Bates, M. J. Carter, P. K. Datta, and R. Hill, *J. Cryst. Growth*, **161**, 148 (1996).
14. S. M. Prokes, W. E. Carlos, L. Seals, S. Lewis, and J. L. Gole, *Mater. Lett.*, **54**, 85 (2002).
15. F. Ochanda and W. E. Jones, *Langmuir*, **21**, 10791 (2005).
16. Y. L. Tai and H. S. Teng, *Chem. Mater.*, **16**, 338 (2004).
17. T. Komiyama, Y. Chonan, J. Onuki, and T. Ohta, *Mater. Trans.*, **43**, 227 (2002).
18. S. Yae, K. Ito, T. Hamada, N. Fukumuro, and H. Matsuda, *Plat. Surf. Finish.*, **92**, 58 (2005).
19. T. Osaka, M. Usuda, I. Koiwa, and H. Sawai, *Jpn. J. Appl. Phys., Part 1*, **27**, 1885 (1988).
20. H. J. Zhang, H. T. Zhang, X. W. Wu, Z. L. Wang, Q. L. Jia, and X. L. Jia, *J. Alloys Compd.*, **419**, 220 (2006).
21. J. Gao, F. Q. Tang, and J. Ren, *Surf. Coat. Technol.*, **200**, 2249 (2005).
22. R. G. Freeman, K. C. Grabar, K. J. Allison, R. M. Bright, J. A. Davis, A. P. Guthrie, M. B. Hommer, M. A. Jackson, P. C. Smith, D. G. Walter, and M. J. Natan, *Science*, **267**, 1629 (1995).
23. L. H. Lu, R. Capek, A. Kornowski, N. Gaponik, and A. Eychmuller, *Angew. Chem., Int. Ed.*, **44**, 5997 (2005).